Effect of pressure on the refractive index of Ge and GaAs

A. R. Goñi, K. Syassen, and M. Cardona
Max-Planck-Institut für Festkörperforschung, Heisenbergstrasse 1, Postfach 80 06 65, D-7000 Stuttgart 80, Federal Republic of Germany
(Received 6 November 1989)

We have measured the dispersion of the refractive index $n(\omega)$ of Ge and GaAs between 0.6 and 1.4 eV for hydrostatic pressures up to 8 GPa. The frequency dependence of $n(\omega)$ is extrapolated to zero energy by using an oscillator model of the dielectric function. In this way, we obtain the variation with pressure of the electronic static dielectric constant ϵ_∞. We find that for the volume change of $\Delta V/V_0 \approx 8\%$ covered in this experiment the volume dependence of ϵ_∞ is well described by a single scaling coefficient $r = d\ln\epsilon_\infty / d\ln V$ with $r = 1.58(3)$ for Ge and 0.73(4) for GaAs. Results are discussed in relation to semiempirical theoretical models.

INTRODUCTION

The dielectric function $\epsilon(\omega)$ at photon energies below the direct optical gap is one of the fundamental properties in the optics of tetrahedral semiconductors. In particular, the dielectric constant in the low-frequency limit, ϵ_∞, appears as an important parameter in related fields like charge screening and other collective phenomena (exciton formation, plasmons, etc.), and in lattice-dynamical properties (Brillouin effect, polarons, and phonon -polaritons). Many of these phenomena are also studied under external hydrostratic pressures and thus the pressure dependence of ϵ_∞ enters into the analysis of the corresponding experimental data. In addition, the pressure dependence of the low-frequency dielectric constant plays an important role in semiempirical models of semiconductor properties under pressure.[1-4] Experimentally, the pressure-induced variation of ϵ_∞ of some important semiconductors such as Ge and GaAs has been obtained from refractive-index measurements at photon energies below the direct gap.[5-9] The available experimental data were mostly obtained using large-volume pressure cells (except those of Ref. 6) and thus are limited to the range below 1 GPa, which does not allow us to determine second-order pressure coefficients. More recently, attempts were made to calculate the volume dependence of ϵ_∞ from first principles.[10,11]

In this paper we report the pressure dependence of the refractive index and its dispersion $n(\omega)$ of Ge and the isoelectronic compound GaAs for pressures up to 8 GPa and in the spectral range between 0.6 and 1.4 eV. We use a simple two-band model of the dielectric function to fit the experimental data, allowing us to obtain the values of the static dielectric constant ϵ_∞ by extrapolation. The pressure and volume dependence of ϵ_∞ is found to be about three times weaker for GaAs than for Ge. This difference is attributed to the partly ionic character of GaAs. A preliminary account of this work has been published in Ref. 12.

EXPERIMENT

The refractive index $n(\omega)$ at $T = 300$ K was measured by an interference method, i.e., by analyzing the interference pattern in the wavelength-dependent transmission of samples with plane-parallel surfaces. The conditions for constructive interference of light transmitted at normal incidence through a plane-parallel sample are given by

$$2dn(\lambda_m) = m\lambda_m \ , \tag{1}$$

where d is the sample thickness, m the order of the interference, and λ_m the wavelength of the corresponding interference maximum. Samples of about $200 \times 200\ \mu m^2$ size were prepared by mechanical polishing of Ge and GaAs single crystals down to thicknesses ranging from 8 to 15 μm. The samples were loaded into a gasketed diamond-anvil cell using a 4:1 methanol-ethanol mixture as a hydrostatic pressure medium.[13] Pressure was measured by the ruby luminescence method.[14] A microoptical system was used to focus white light from a tungsten lamp onto the sample and to collect the transmitted intensity, focusing it onto the slits of a 0.25-m single-grating monochromator. The light was detected with a cooled PbS cell and the signal recorded by conventional synchronous detection. Lines of a Kr discharge lamp were used to ensure the reproducibility of the wavelength calibration.

Representative transmission spectra of Ge measured at two different pressures are shown in Fig. 1. The interference pattern is clearly observed below the direct absorption edge at energy E_0. The assignment of the order m for each maximum was performed at ambient pressure from the wavelength separation $\lambda_m - \lambda_{m+1}$ between two consecutive maxima and by using $n(\omega)$ data tabulated in Ref. 15. The sample thickness at ambient pressure was then determined from the wavelengths of the interference maxima in the zero-pressure spectra (about 15 maxima for Ge and 50 for GaAs were evaluated). We kept track of the numbering of each maximum during a whole pres-

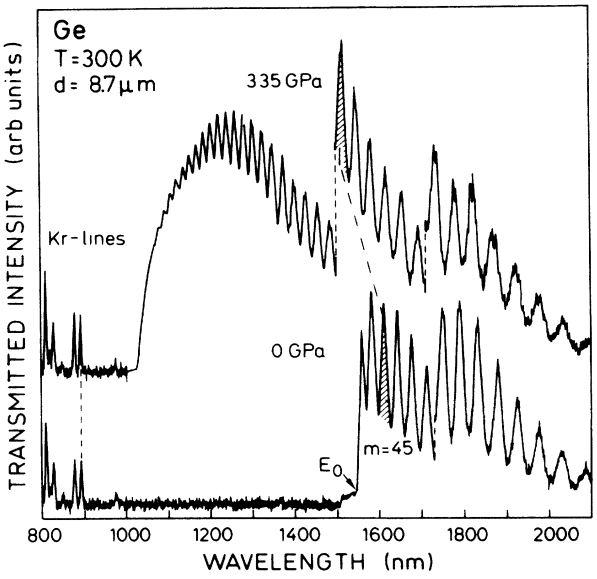

FIG. 1. Near-infrared transmission spectra of an 8.7-μm-thick Ge sample at two different pressures. The interference of order $m=45$ is shown to shift to lower wavelengths with increasing pressure (see text for details).

sure cycle by recording the number of maxima passing by at a fixed wavelength, when the pressure was changed. For this purpose an electric motor drive was used to change the pressure in a continuous manner and at low speed (by ~ 0.5 kbar/min).

In Fig. 1 the pressure shift of the interference maximum of order 45 is indicated. For the high-pressure spectra we again use Eq. (1) to calculate $n(\omega)$, but also take into account the thickness reduction by scaling d using the Murnaghan's equation of state:[16]

$$d(P)/d_0=(1+B_0'P/B_0)^{-1/3B_0'} . \quad (2)$$

The values used for the isothermal bulk modulus and its pressure derivative are $B_0=74.4$ GPa, $B_0'=4.76$ for Ge (Ref. 17) and $B_0=74.7$ GPa, $B_0'=4.46$ for GaAs (Ref. 18), respectively. We took special care in always illuminating the same region of the sample to avoid possible errors due to changes in the thickness because of nonparallelism of the sample surfaces. The effect of a possible small tilting of the sample in the pressure cell is negligible, because the effective thickness of the sample when tilted by an angle ϑ changes like $\cos\vartheta$ and ϑ is always less than 0.1 rad. In this way, it was possible to determine the refractive index at high pressure with an estimated error of less than 0.3%.

Some representative data for $n(\omega)$ of Ge and GaAs measured at several pressures are shown in Fig. 2 (solid circles). The scatter of the data points is mainly caused by uncertainities in the determination of the maximum positions λ_m, due to spurious interferences coming from multiple reflections inside the pressure cell. It is clear from Figs. 2(a) and 2(b) that the pressure effects on $n(\omega)$ are much stronger for Ge than for GaAs. Near 0.6 eV this difference amounts to a factor of 3. In the case of Ge, $n(\omega)$ decreases more drastically in the immediate vicinity of the direct gap E_0 a consequence of the blue shift of the E_0 band gap under pressure.[19]

REFRACTIVE-INDEX DISPERSION

The refractive-index dispersion and its pressure dependence in Ge and GaAs is described by a two-oscillator model of the complex dielectric function $\epsilon(\omega)=\epsilon_1(\omega)+i\epsilon_2(\omega)$, which is a slightly modified version of the model of Refs. 20 and 21. Below the E_0 gap the absorption coefficient vanishes (the indirect absorption is negligible) and the refractive index is simply given by $n(\omega)=\sqrt{\epsilon_1(\omega)}$. The main contribution to $\epsilon_1(\omega)$ below the

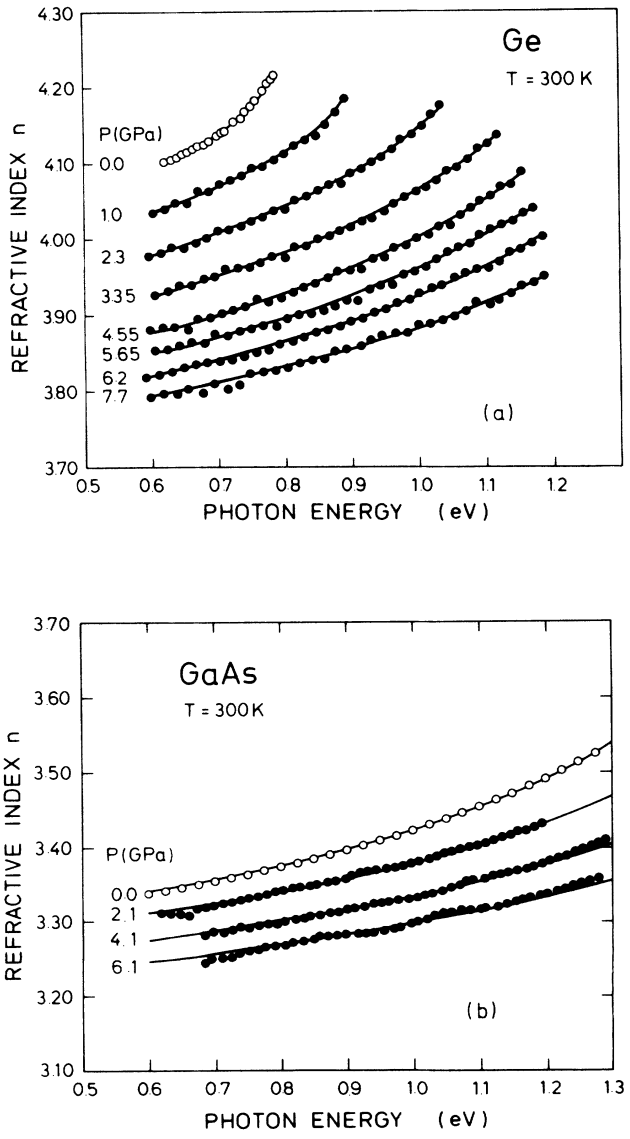

FIG. 2. The refractive index of (a) Ge and (b) GaAs as a function of photon energy at several pressures (solid circles). Open circles are literature data (Ref. 15) of $n(\omega)$ at normal pressure. The solid curves represent the result of fitting a two-oscillator model to the experimental data.

direct optical gap is generated by a band of oscillators associated with the two-dimensional critical point (CP) at energy E_1, which corresponds to the energy of interband transitions along the Γ-L direction. A cutoff energy E_c is introduced in order to avoid unphysical extension of this oscillator response to high energies. Furthermore, we include transitions at the three-dimensional interband minimum at point Γ corresponding to the lowest direct optical gap E_0, with an additional δ-like Lorentz oscillator to account for the discrete exciton. Details are given in the Appendix.

The oscillator model for $\epsilon(\omega)$ of Ge at ambient pressure is illustrated in Fig. 3. The function $\epsilon_2(\omega)$ is given by the combination of Eqs. (A1), (A3), and (A5), while $\epsilon_1(\omega)$ is obtained using Eqs. (A2), (A4), and (A6). The model has only two adjustable parameters C_0'' and B, corresponding to the oscillator- strength of transitions at energies E_0 and E_1. The other parameters used are listed in Table I. The main difference with respect to previous reports[21,28] is that we take into account sum-rule considerations, such that the cutoff frequency E_c, which is of the order of the valence-electron plasma frequency, is determined through the parameters C_0'' and B by the ϵ_2 sum rule. For comparison, we also show in Fig. 3 the experimental $\epsilon_2(\omega)$.[22] The strong critical-point transition E_2 (corresponding to interband transitions along the Γ-X direction) does not appear explicitly in the model, but its contribution to $\epsilon_1(\omega)$ in the region below the direct gap is retained due to the sum-rule constraints (see the Appendix).

For the analysis of high-pressure data we take into account the experimental dependence of the E_0 and E_1 band gaps on pressure (see Table I). By imposing the validity of the static sum rule [Eq. (A9)] at higher pressures, the pressure coefficient of the cutoff frequency E_c turns out to be the same as for the E_1 gap. The results of least-squares fits to the experimental $n(\omega)$ data are shown by the solid lines in Fig. 2(a) and 2(b). For all pressures

TABLE I. List of parameters used in fitting the oscillator model (see text) to the experimental $n(\omega)$ data of Ge and GaAs. They are the energy positions of the oscillators, E_0 and E_1, and that pressure coefficients, the spin-orbit splitting Δ_0, the cutoff energy E_c at zero pressure, the excitonic oscillator strength A, and the effective number of valence electrons, N_{eff}.

	Ge	GaAs
E_0 (eV)	0.8[a]	1.43[b]
dE_0/dP (eV) GPa^{-1})	0.121[a]	0.108[b]
Δ_0 (eV)	0.29[c]	0.34[c]
E_1 (eV)	2.14[d]	2.89[e]
dE_1/dP (eV GPa^{-1})	0.088[d]	0.074[e]
$E_c(P=0)$ (eV)	17.5	14.5
A (a.u.)	0.004	0.013
N_{eff}	5[f]	4.3[f]

[a]Reference 19.
[b]Reference 23.
[c]Reference 24.
[d]Reference 25.
[e]Reference 26.
[f]Reference 27.

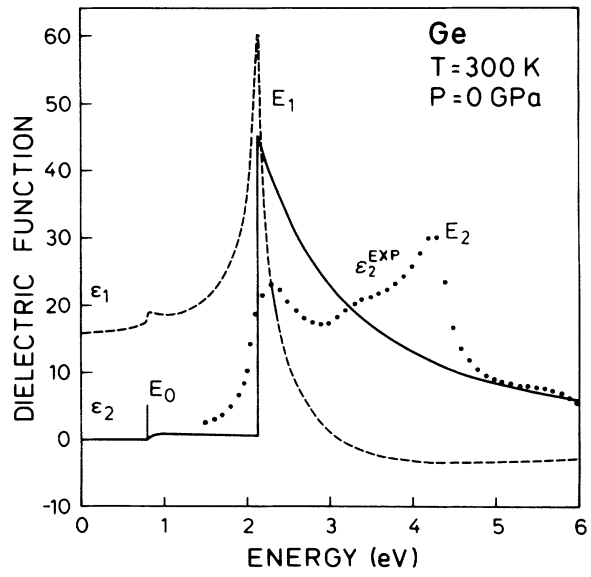

FIG. 3. Real and imaginary part of the model dielectric function used to describe the refractive-index dispersion in Ge at ambient pressure. The dotted curve represents experimental data from Ref. 22.

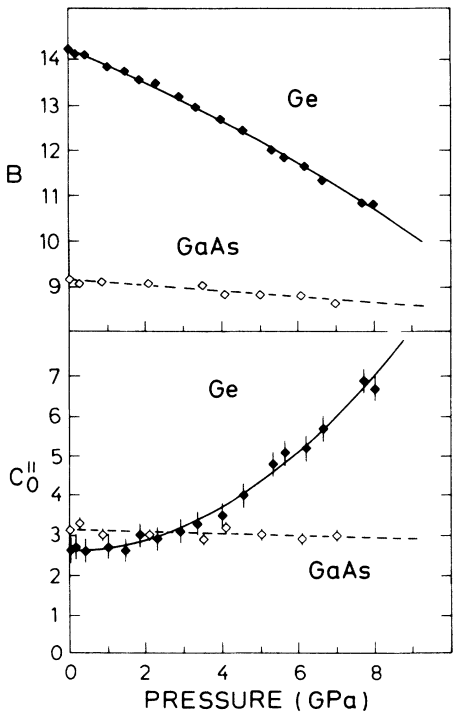

FIG. 4. The parameters B and C_0'' obtained by fitting the model dielectric function to the experimental data of $n(\omega)$. The lines correspond to least-squares fits using linear and quadratic expressions.

the model function provides an excellent description of the experimental refractive-index dispersion.

In Fig. 4 we have plotted the values of the parameters B and C_0'', which give the best fit to the $n(\omega)$ data. The lines in Fig. 4 represents fits with linear or quadratic expressions giving the following coefficients:

$$[B(P)]_{\mathrm{Ge}}=14.24(3)-0.35(2)P-0.012(2)P^2\ ,$$
$$[C_0''(P)]_{\mathrm{Ge}}=2.6(1)+0.068(7)P^2\ ; \tag{3a}$$

$$[B(P)]_{\mathrm{GaAs}}=9.14(4)-0.07(1)P\ ,$$
$$[C_0''(P)]_{\mathrm{GaAs}}=3.1(1)-0.03(2)P\ . \tag{3b}$$

Using these coefficients the set of Eqs. (A2), (A4), and (A6) and the band-gap parameters listed in Table I one can obtain the refractive index of Ge and GaAs as a function of pressure for a given photon energy below the direct optical-absorption edge.

The B values of Eqs. (3a) and (3b) are roughly a factor of 2 larger than the theoretical estimates for the E_1 transition ($B=7.32$ and 5.43 a.u. for Ge and GaAs, respectively[21]). This difference is a consequence of the N_{eff} sum rule [see Eq. (A8)] imposed on the model function. In this way, the oscillator strength corresponding to the E_2 peak is in part accounted for in the magnitude of B and the cutoff E_c. The strength C_0'' of the oscillator at E_0 is again a factor of 2 larger than the theoretical prediction. In this case, we attribute the enhancement observed in the experiment to the exciton formation, which steepens the absorption edge at E_0, an effect that is not completely accounted for in our model by introducing a Lorentz oscillator.

PRESSURE AND VOLUME DEPENDENCE OF ϵ_∞

We use the above-described model of the dielectric properties to extrapolate the frequency dependence of $n(\omega)$ to zero energy in order to obtain the variation of $\epsilon_\infty \approx n^2(\omega\rightarrow 0)$ as a function of pressure, as shown in Fig. 5(a). The lines through the data points in Fig. 5(a) correspond to the results of least-squares fits (P in GPa):

$$[\epsilon_\infty(P)]_{\mathrm{Ge}}=15.94(2)-0.36(2)P+0.014(2)P^2\ ,$$
$$[\epsilon_\infty(P)]_{\mathrm{GaAs}}=10.92(2)-0.088(4)P\ .$$

At ambient pressure we obtain for ϵ_∞ the values given in the literature[15,24] to within 0.5%. A strong nonlinear pressure dependence of ϵ_∞ is observed for Ge and the corresponding linear coefficient is about four times larger than that of GaAs.

Figure 5(b) shows the dependence of ϵ_∞ on volume. The double-logarithmic plot demonstrates that a single-scaling coefficient $r=d\ln\epsilon_\infty/d\ln V$ is sufficient to describe the volume dependence of ϵ_∞. The values of r obtained here for Ge and GaAs are listed in Table II together with other experimental and theoretical results. Values of r from previous experiments (mostly studies up to 1.5 GPa) agree within 20% with our results obtained for a larger range of pressures. The empirical dielectric Phillips–Van Vechten theory[1,2] and an empirical pseudopotential calculation[4] produce results that are close to the experimental value. Recently developed first-principles linear muffin-tin orbitals (LMTO) calculations, which successfully reproduce the main features of the spectral dependence of the dielectric function,[10] give unsatisfactory results for the static limit. That might be due to the

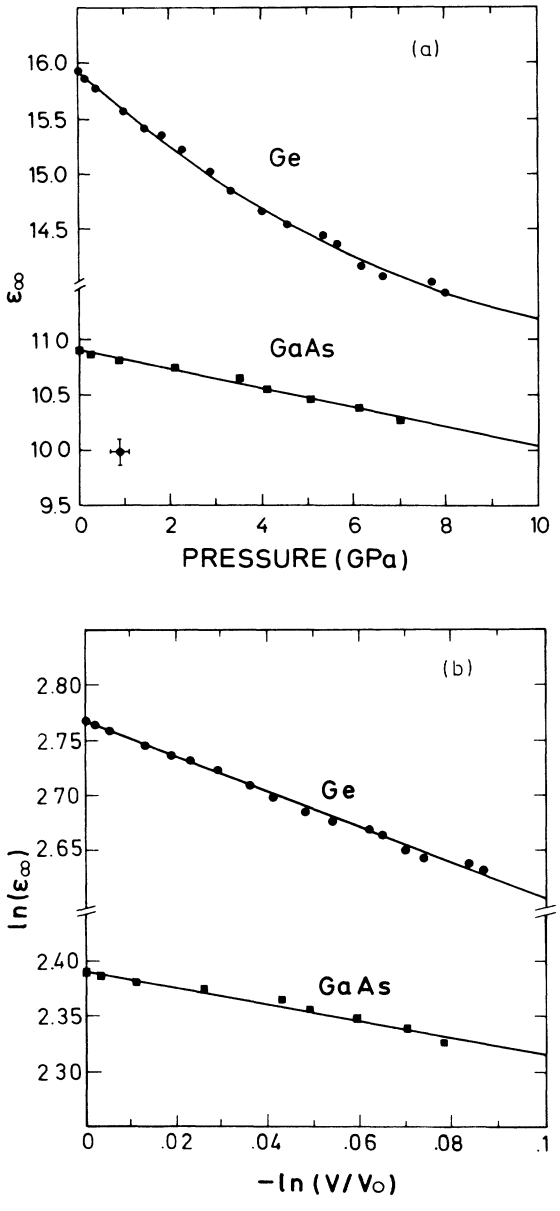

FIG. 5. (a) The static dielectric constant of Ge and GaAs as a function of pressure obtained by extrapolation of the frequency dependence of $n(\omega)$ to zero energy. The lines represent fits to the data points with linear and quadratic functions. (b) Double-logarithmic plot of the static dielectric constant of Ge and GaAs vs volume.

fact that d electrons, which play an important role in the optical properties of Ge and GaAs, are not taken into account.

The behavior of the dielectric function under pressure differs drastically for ionic and covalent materials, as illustrated by the examples of ionic crystals also listed in Table II. In the case of ionic materials (NaCl), ϵ_∞ increases with pressure. A simple way to explain this difference starts from the Sellmeyer formula:[31] $\epsilon_\infty = 1 + 4\pi N\alpha_p$, which relates ϵ_∞ to the microscopic polarizability α_p per primitive unit cell in the case of N delocalized dipoles per unit volume. The volume derivative of that relation gives[32]

$$r = \partial \ln \epsilon_\infty / \partial \ln V \sim -(1 - \partial \ln \alpha_p / \partial \ln V) \ . \quad (4)$$

In large-band-gap ionic materials like the alkali halides α_p changes very little with pressure. Consequently, the changes of the macroscopic dielectric constant with pressure are governed by the increase in the density of polarizable centers giving negative values for r. On the contrary, in covalent semiconductors the bond polarizability depends strongly on bond length. In this case, large changes in the polarizability α_p are responsible for the observed decrease of ϵ_∞ with pressure. This effect is expected to be less pronounced for materials with a partly ionic character of the chemical bond which thus provides a qualitative explanation for the smaller pressure dependence of ϵ_∞ in GaAs as compared to Ge.

Within the Penn gap model[33] and the dielectric theory of the covalent bond of Phillips and Van Vechten[2] the static dielectric constant is given by

$$\epsilon_\infty = 1 + DA\omega_p^2 / E_g^2 \quad \text{with } E_g^2 = E_h^2 + C^2 \ . \quad (5)$$

Here, ω_p is the valence-electron plasma frequency and E_g is the average optical gap (or Penn gap), which splits into a homopolar (covalent) contribution E_h and a ionic contribution C. The factor A is constant ($A \sim 1$) and $D = N_{\text{eff}}/4$ accounts for the effects of occupied d states on the interband transition probability. The plasma frequency varies as $\omega_p \sim V^{-1/2}$, and it is generally assumed[1,2] that $dC/dP \approx 0$. The volume dependence of E_h and D is estimated to be $E_h \sim V^{0.83}$ (Ref. 2) and $D - 1 \sim V^{4.3}$ (Ref. 1). The volume derivative of ϵ_∞ can be then written in terms of the Phillips–Van Vechten ionicity $f_i = C^2/E_g^2$ as

$$\partial \ln \epsilon_\infty / \partial \ln V \approx \frac{5(\epsilon_\infty - 1)}{3\epsilon_\infty}(0.9 - f_i) \ . \quad (6)$$

According to Eq. (6) the borderline between a "covalent" and "ionic" volume dependence of ϵ_∞ (corresponding to a change in the sign of r) is given by $f_i \approx 0.9$. Using Eq. (6) and the ionicities listed in Table II we estimate for Ge and GaAs the values of $r = \partial \ln \epsilon_\infty / \partial \ln V = 1.43$ and 0.91,

TABLE II. Pressure and volume coefficients of the refractive index $n(\omega = 0)$ and static dielectric constant, respectively, for Ge, GaAs, GaP, and NaCl. The bulk modulus B_0 is used to transform from pressure to volume coefficients. The Phillips ionicity (Ref. 2) f_i of each material is also listed.

Sample (f_i)	ϵ_∞	B_0 (GPa)	$\left[\frac{\partial\omega}{\partial P}\right]_{\omega=0}$ (10^{-2} GPa^{-1})	$\frac{\partial \ln \epsilon_\infty}{\partial \ln V} = r$	Reference
Ge (0)	15.94(2)	74.4	−4.5(2)	1.58(3)	Expt.: This work, transmission, diamond anvil cell (DAC)
			−5.6(5)	2.0(1)	Expt.: Ref. 5, transmission ($P < 0.3$ GPa)
			−5.8	2.1	Expt.: Ref. 9, stress-birefringence ($\lambda = 11$ μm)
		75.2	−2.8(8)	1.1(2)	Expt.: Ref. 8
	16	75.2	−4	1.50	Theor.: Ref. 1, dielectric theory
	16	75.2	−3.56	1.34	Theor.: Ref. 4, empirical pseudopotential
	21.9	74.4		1.6	Theor.: Ref. 11, Penn model (Two Baldereschi special **k** points)
	14.08			2.83	Theor.: Ref. 10, *ab initio* LMTO
GaAs (0.31)	10.92(2)	74.7	−1.3(1)	0.73(4)	Expt.: This work, transmission, DAC
		74.7	−1.9(2)	0.82(6)	Expt.: Ref. 6, reflection, DAC
	11.56	74.6	−2.4(3)	1.04(15)	Expt. cited in Ref. 1
	11.56		−1.70	0.75	Theor.: Ref. 1, dielectric theory
	10.9	74.6	−1.45	0.66	Theor.: Ref. 4, empirical pseudopotential
	15.3			1.20	Theor.: Ref. 11, Penn model (Two Baldereschi special **k** points)
	12.95			1.68	Theor : Ref. 10, *ab initio* LMTO
GaP (0.37)	9.50(1)	88.1	−1.1(2)	0.63(8)	Expt.: Ref. 21, transmission, DAC
	9.0	88.5	−0.9	0.53	Theor.: Ref. 1, dielectric theory
NaCl (0.94)	2.25	24	1.17	−0.37	Expt.: Ref. 29
	2.61			−0.88	Theor.: Ref. 30

respectively, in reasonable agreement with the experimental results (see Table II).

SUMMARY

In summary, the refractive index $n(\omega)$ of Ge and GaAs, measured in the energy range below the direct absorption edge E_0 up to 8 GPa, decreases monotonically with increasing pressure. The relative change $d\ln(n)/dP$ is more pronounced for Ge than for GaAs. The static dielectric constant ϵ_∞ is extrapolated from the frequency dependence of $n(\omega)$ to zero energy using an empirical oscillator model. For a 8% volume change covered in this experiment we find that the volume dependence of ϵ_∞ is well described by a single-scaling coefficient $r=\partial\ln\epsilon_\infty/\partial\ln V$ with $r=1.58(3)$ and 0.73(4) for Ge and GaAs, respectively. Theoretical estimates based on semiempirical models[1,4] are in good agreement with these experimental results. The significant difference in the volume coefficient of ϵ_∞ for Ge and GaAs is attributed to the ionicity difference.

ACKNOWLEDGMENTS

We thank W. Böhringer, W. Dieterich, and R. Hempel for technical assistance.

APPENDIX

In this appendix we summarize the empirical model[21] of the dielectric function $\varepsilon(\omega)$ used to describe the dispersion of the refractive index of Ge and GaAs at energies below the fundamental direct optical gap E_0. The main contributions to $\epsilon_2(\omega)$ in tetrahedral semiconductors arise from transitions related to Van Hove singularities at *critical points* (CP) in the joint density of states in the Γ-L direction (E_1 gap) and near the X point (E_2 gap) of the Brillouin zone.[22,34] In our model these two contributions are combined into a single oscillator at energy E_1.

The critical point associated with transitions at the E_1 gap is of P_0 type.[35] Because of the large difference between the longitudinal and the transverse effective masses, one can treat this CP as two dimensional.[28] Hence, the contribution to the imaginary part of the dielectric constant is

$$\Delta\epsilon_2(\omega)=\begin{cases}\pi B/X_1^2 & \text{for } E_1<\hbar\omega<E_c\\ 0 & \text{otherwise},\end{cases} \tag{A1}$$

with $X_1=\hbar\omega/E_1$. The cutoff energy E_c is introduced to fulfill optical sum rules (see below). The Kramers-Kronig transformation of Eq. (A1) can be obtained analytically,[20] leading to

$$\Delta\epsilon_1(\omega)-1=-\frac{B}{X_1^2}\ln\left[\frac{1-X_1^2}{1-X_c^2}\right],\quad X_c=\hbar\omega/E_c\ . \tag{A2}$$

Transitions at E_0 produce strong dispersion of $n(\omega)$ in the vicinity of the direct gap. This CP is identified as a three-dimensional interband minimum (M_0 type) and, assuming parabolic bands, $\epsilon_2(\omega)$ behaves as a square-root-like edge:

$$\Delta\epsilon_2(\omega)=\begin{cases}C_0''(X_0^{-2}\sqrt{X_0-1}+0.43X_{\rm os}^{-2}\sqrt{X_{\rm os}-1}) & \text{for } \hbar\omega>E_0,\ E_0+\Delta_0\\ 0, \text{ otherwise},\end{cases} \tag{A3}$$

with $X_0=\hbar\omega/E_0$ and $X_{\rm os}=\hbar\omega/(E_0+\Delta_0)$, where Δ_0 is the spin-orbit splitting of the valence band at the Γ point. For ϵ_1 one gets

$$\Delta\epsilon_1(\omega)=C_0''[f(X_0)+0.433f(X_{\rm os})] \tag{A4a}$$

with

$$f(X)=X^{-2}[2-\sqrt{1+X}-\sqrt{1-X}\,\Theta(1-X)] \tag{A4b}$$

(Θ is the unit-step function). The value of C_0'' was calculated in Ref. 20 (without taking into account excitonic effects) to be 1.9 for Ge and 1.6 for GaAs.

To account for the discrete exciton at the direct gap energy E_0, we add a δ-function-like Lorentz oscillator:

$$\Delta\epsilon_2(\omega)=A\,\delta(\hbar\omega-E_0)\ , \tag{A5}$$

$$\Delta\epsilon_1(\omega)=\frac{A}{1-X_0^2}\ . \tag{A6}$$

We assume for A the value predicted by the exciton theory of Elliott[36] which, in atomic units, is

$$A=\frac{32P^2\mu^3}{3\epsilon_\infty^3E_0^3}\sum_{m=1}^{\infty}\frac{1}{m^3}\ . \tag{A7}$$

Here $P\approx 2\pi/a$ (a is the lattice parameter) is the momentum matrix element, μ is the reduce effective mass, and the summation runs over all discrete exciton levels. From Eq. (A7) we obtain $A=0.004$ for Ge and 0.013 for GaAs.

The total oscillator strength, i.e., adding the contributions of all interband transitions with energies up to the plasma frequency ω_p, must remain finite to fulfill the corresponding sum rule for the effective number $N_{\rm eff}$ of valence electrons contributing to the optical response:[15]

$$N_{\rm eff}(\omega_p)=\frac{m}{2\pi^2e^2}\int_0^{\omega_p}\omega\epsilon_2(\omega)d\omega\ , \tag{A8}$$

where m and e are the free-electron mass and charge. Equation (A8) imposes a constraint to the two oscillator strengths C_0'' and B and the cutoff energy E_c, so that they cannot be varied arbitrarily. In order to determine uniquely the cutoff E_c in terms of the two oscillator strengths we also require the validity of the static sum rule:

$$\epsilon_\infty-1=\frac{2}{\pi}\int_0^{E_c}\frac{\epsilon_2(\omega)}{\omega}d\omega\ . \tag{A9}$$

Now the interplay between B and the cutoff E_c is given by the application of both sum rules.

[1]D. L. Camphausen, G. A. N. Connell, and W. Paul, Phys. Rev. Lett. **26**, 184 (1971).
[2]J. A. Van Vechten, Phys. Rev. **182**, 891 (1969).
[3]M. Kastner, Phys. Rev. B **6**, 2273 (1972).
[4]Y. F. Tsay, S. S. Mitra, and B. Bendow, Phys. Rev. B **10**, 1476 (1974).
[5]N. J. Trappeniers, R. Vetter, and H. A. R. de Bruin, Physica (Amsterdam) **45**, 619 (1970).
[6]M. Manfland, Master of Physics thesis, Düsseldorf University, 1985 (unpublished).
[7]W. M. DeMeis, Gordon McKay Laboratory Technical Report No. HP-15, Harvard University, 1965 (unpublished).
[8]M. Cardona, W. Paul, and H. Brooks, J. Phys. Chem. Solids **8**, 204 (1959).
[9]A. Feldmann, R. M. Waxler, and D. Horowitz, J. Appl. Phys. **49**, 2589 (1978).
[10]M. Alouani, L. Brey, and N. Christensen, Phys. Rev. B **37**, 1167 (1988).
[11]M. Cardona and S. Gopalan, in *Progress in Electron Properties of Solids,* edited by R. Girlanda *et al.* (Kluwer, Amsterdam, 1989).
[12]A. R. Goñi, K. Syassen, K. Strössner, and M. Cardona, Semicond. Sci. Technol. **4**, 246 (1989).
[13]S. Hawke, K. Syassen, and W. Holzapfel, J. Sci. Instrum. **45**, 1548 (1974).
[14]H. K. Mao and P. M. Bell, Science **200**, 1145 (1978).
[15]E. D. Palik in *Handbook of Optical Constants of Solids,* edited by E. D. Palik (Academic, New York, 1985).
[16]F. D. Murnaghan, Proc Natl. Acad. Sci. USA **30**, 244 (1944).
[17]H. J. McSkimin and P. Andreatch, Jr., J. Appl. Phys. **34**, 651 (1963).
[18]H. J. McSkimin, A. Jayaraman, and P. Andreatch, J. Appl. Phys. **38**, 2362 (1967).
[19]A. R. Goñi, K. Syassen, and M. Cardona, Phys. Rev. B **39**, 12 921 (1989).
[20]M. Cardona, in *Atomic Structure and Properties of Solids,* edited by E. Burstein (Academic, New York, 1972).
[21]K. Strössner, S. Ves, and M. Cardona, Phys. Rev. B **32**, 6614 (1985).
[22]D. E. Aspnes and Studna, Phys. Rev. B **27**, 985 (1983).
[23]A. R. Goñi, K. Strössner, K. Syassen, and M. Cardona, Phys. Rev. B **36**, 1581 (1987).
[24]*Numerical Data and Functional Relationships in Science and Technology,* Vol. 17a of *Landolt-Börnstein,* New Series, edited by O. Madelung, H. Weiss, and M. Schulz (Springer, Heidelberg, 1982).
[25]M. Kobayashi, T. Nagahama, and Y. Nisida, in *Proceedings of the 18th International Conference on the Physics of Semiconductors, Stockholm, 1986,* edited by O. Engström (World Scientific, Singapore, 1986).
[26]M. Hanfland, K. Syassen, and N. Christensen; J. Phys. (Paris) Colloq. **45**, C8-57 (1984).
[27]H. R. Philipp and H. Ehrenreich, Phys. Rev. **129**, 1550 (1963).
[28]S. Adachi, Phys. Rev. B **35**, 7454 (1987).
[29]J. Fontanella, C. Andeen, and D. Schuele, Phys. Rev. B **6**, 582 (1972).
[30]J. Shanker, V. P. Gupta, and O. P. Sharma, Phys. Rev. B **18**, 5869 (1978).
[31]P. Nozières and D. Pines, Phys. Rev. **109**, 762 (1958).
[32]G. A. Samara, Phys. Rev. B **27**, 3494 (1983).
[33]D. R. Penn, Phys. Rev. **128**, 2093 (1962).
[34]M. L. Cohen and J. R. Chelokowsky, *Electronic Structure and Optical Properties of Semiconductors* (Springer, Heidelberg, 1988).
[35]F. Bassani and M. Altarelli, in *Handbook of Synchrotron Radiation,* edited by E. E. Koch (North-Holland, Amsterdam, 1983), Vol. 1.
[36]R. J. Elliott, Phys. Rev. **108**, 1384 (1957); P. Y. Yu and M. Cardona, J. Phys. Chem. Solids **34**, 29 (1973).